

Intratumoral electroporation of a self-amplifying RNA expressing IL-12 induces antitumor effects in mouse models of cancer

Noelia Silva-Pilipich,^{1,3,4} Aritz Lasarte-Cía,^{2,3,4} Teresa Lozano,^{2,3} Celia Martín-Otal,^{2,3} Juan José Lasarte,^{2,3} and Cristian Smerdou^{1,3}

¹Division of Gene Therapy and Regulation of Gene Expression, Cima Universidad de Navarra, Av. Pío XII 55, 31008 Pamplona, Spain; ²Program of Immunology and Immunotherapy, Cima Universidad de Navarra, Av. Pío XII 55, 31008 Pamplona, Spain; ³Instituto de Investigación Sanitaria de Navarra (IdISNA), Pamplona, Spain

Alphavirus vectors based on self-amplifying RNA (saRNA) generate high and transient levels of transgene expression and induce innate immune responses, making them an interesting tool for antitumor therapy. These vectors are usually delivered as viral particles, but it is also possible to administer them as RNA. We evaluated this possibility by *in vivo* electroporation of Semliki Forest virus (SFV) saRNA for local treatment of murine colorectal MC38 subcutaneous tumors. Optimization of saRNA electroporation conditions in tumors was performed using an SFV vector coding for luciferase. Then we evaluated the therapeutic potential of this approach using an SFV saRNA coding for interleukin-12 (SFV-IL-12), a proinflammatory cytokine with potent antitumor effects. Delivery of SFV-IL-12 saRNA by electroporation led to improvement in tumor control and higher survival compared with mice treated with electroporation or with SFV-IL-12 saRNA alone. The antitumor efficacy of SFV-IL-12 saRNA electroporation increased by combination with systemic PD-1 blockade. This therapy, which was also validated in a hepatocellular carcinoma tumor model, suggests that local delivery of saRNA by electroporation could be an attractive strategy for cancer immunotherapy. This approach could have easy translation to the clinical practice, especially for percutaneously accessible tumors.

INTRODUCTION

Over the last decade, there have been spectacular advances in the field of cancer immunotherapy. Discovery of checkpoint inhibitors of the immune system, with subsequent development of specific blocking antibodies, bispecific antibodies, adoptive cell therapies, or use of cytokines, has allowed us to face cancer from a different perspective where therapies exploit the ability of immune cells to recognize and kill tumor cells.¹

Despite these advances, there are still many types of tumors that do not respond to immunotherapies. The complexity of the tumor stroma, its aberrant vasculature, metabolic restrictions, recruitment of immunosuppressive cells to the tumor bed, and generation of an immunosuppressive microenvironment are among the great obsta-

cles the immune system must face for its antitumor action.² Locoregional therapies, including radiotherapy,³ radiofrequency,⁴ microwave ablation,⁵ thermal ablation,⁶ radioembolization,⁷ or irreversible electroporation,⁸ besides their direct effect on tumor cells, may also have an effect on the hostile tumor microenvironment that is unfavorable for the antitumor activity of the immune system. However, these techniques do not adequately transform this highly immunosuppressive microenvironment. For this reason, locoregional therapies are being combined with other immunostimulatory therapies, such as use of anti-checkpoint antibodies,^{3,6,9} immunological adjuvants, such as poly(I:C)^{10,11} or STING agonists,¹² delivery of tumor suppressor genes,¹³ oncolytic viruses,¹⁴ or cytokines.¹⁵

One of the most effective antitumoral cytokines is interleukin-12 (IL-12), which mediates its antitumor activity through stimulation of T, natural killer (NK), and NK T cells and through its antiangiogenic effect.^{16,17} However, systemic IL-12 expression may cause toxicity because of induction of high levels of interferon (IFN)- γ .¹⁸ Strategies allowing local expression of IL-12 in tumors (i.e., by using viral vectors encoding the cytokine) have been developed, giving rise to high antitumoral efficacy with reduced toxicity.¹⁹ Nevertheless, therapeutic strategies based on replicative viruses are not without risks, and regulatory limitations make it difficult to translate them into clinical practice. In this scenario, use of non-viral vectors, specifically RNA vectors, is gaining a lot of interest because of their recent results with anti-viral and anti-tumor vaccination strategies.²⁰ RNA based therapies are showing important expression capacity and very promising safety profiles for their application to different therapeutic

Received 18 January 2022; accepted 15 July 2022;
<https://doi.org/10.1016/j.omtn.2022.07.020>

⁴These authors contributed equally

Correspondence: Cristian Smerdou, Division of Gene Therapy and Regulation of Gene Expression (CS) or Program of Immunology and Immunotherapy (JLL), Cima Universidad de Navarra, Av. Pío XII 55, 31008 Pamplona, Spain.
E-mail: csmerdou@unav.es

Correspondence: Juan J. Lasarte, Program of Immunology and Immunotherapy (JLL), Cima Universidad de Navarra, Av. Pío XII 55, 31008 Pamplona, Spain.
E-mail: jjlasarte@unav.es



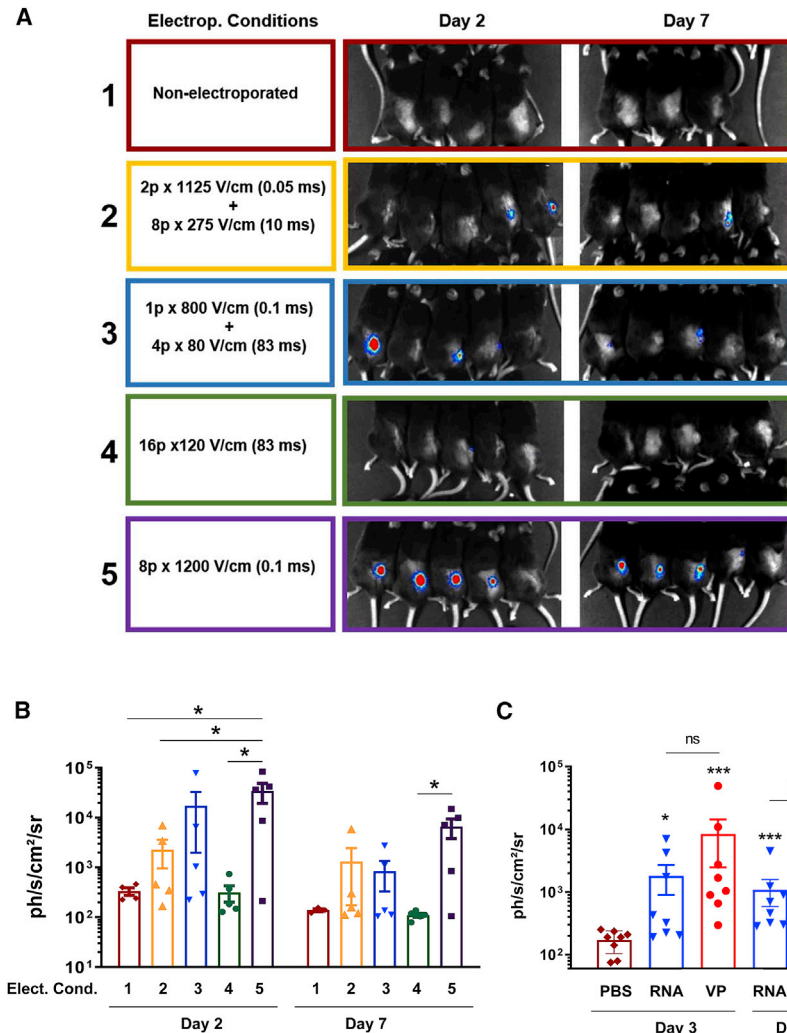


Figure 1. Optimization of electroporation conditions using SFV-Luc saRNA in MC38 subcutaneous tumors

(A) Mice bearing $\sim 30\text{-mm}^3$ MC38 subcutaneous tumors were treated i.t. with $10\ \mu\text{g}$ of SFV-Luc saRNA plus electroporation using the conditions indicated in the left column (p, number of pulses; V/cm, volts/cm; ms, duration of each pulse in milliseconds; pulse interval of 0.5 s for every condition). Control groups received saline solution without electroporation (non-electroporated). All mice were injected with luciferin, and images were acquired with a CCD camera at the indicated times using an exposure time of 2 min. (B) Quantification of light emission in mice shown in (A) (Elect. Cond., electroporation conditions defined in A). (C) Comparison of Luc expression in MC38 tumors electroporated with SFV-Luc saRNA (8 pulses of 0.1 ms at 1,200 V/cm, pulse interval of 0.5 s) (RNA) or injected with 10^8 SFV viral particles (VPs). The control group received PBS and was electroporated using the same conditions as the RNA group. Bioluminescence was measured at the indicated times. Data represent mean measurement of the light emission in photons/s/cm²/sr \pm SEM. Asterisks at the top of each group correspond to comparisons with the PBS control group. Other comparisons are indicated by horizontal lines. * $p < 0.05$; *** $p < 0.001$; ns, not significant.

strategies beyond vaccines. The challenge for these technologies is their formulation to reach target cells at adequate therapeutic levels.²¹ In this work, we explored use of a physical technique based on *in vivo* electroporation to introduce into tumor cells a self-amplifying RNA (saRNA) derived from Semliki Forest virus (SFV) encoding the IL-12 transgene. The SFV vector consists of a single positive-strand RNA that encodes a viral replicase able to self-amplify the viral RNA in the host cell but lacks the genes encoding the viral structural proteins, which are replaced by the transgene of interest. The mRNA coding for the protein of interest is amplified abundantly from a viral subgenomic promoter (sgPr) present in the negative-strand RNA produced during the replication process. Therefore, this system is able to promote very high and transient expression of the transgene, also inducing IFN-I responses and apoptosis of transduced cells.^{22–24} Strong antitumor effects have been observed when SFV saRNA coding for IL-12 (SFV-IL-12) was delivered as viral particles in different cancer preclinical models.^{25–29} In this work, we optimized the intratumor electroporation conditions of SFV saRNA, demonstrating

effective anti-tumor immune responses in murine models of colon and liver cancer when using the SFV-IL-12 vector.

RESULTS

Optimization of intratumoral SFV saRNA delivery by electroporation

We first optimized the electroporation conditions to obtain high gene expression in subcutaneous colon adenocarcinoma tumors (MC38). For this, a reporter vector based on SFV saRNA coding for luciferase (SFV-Luc) was employed. After making a small incision into the skin to expose the tumors, $10\ \mu\text{g}$ of SFV-Luc RNA was injected intratumorally (i.t.), followed immediately by local tumor electroporation using platinum plate tweezer-type electrodes and four different electroporation conditions, as indicated in Figure 1A. These conditions, which varied in the voltage (V/cm), duration, and number of pulses, were selected based on previous studies in which DNA or RNA had been electroporated into skin, muscle, or tumors.^{30–35} The saRNA was supplemented with RNase inhibitor immediately before electroporation because it has been shown recently that this can increase the efficacy and repeatability of saRNA intradermal electroporation.³⁶ On days 2 and 7 after electroporation, bioluminescence was measured in live animals using a charge-coupled device (CCD) camera (Figure 1A, right images). Mice electroporated with eight high-voltage short pulses (1,200 V/cm, pulse length of 0.1 ms, and pulse interval of 0.5 s) showed the highest expression of Luc among all tested conditions (Figure 1B). Despite the transient nature of the

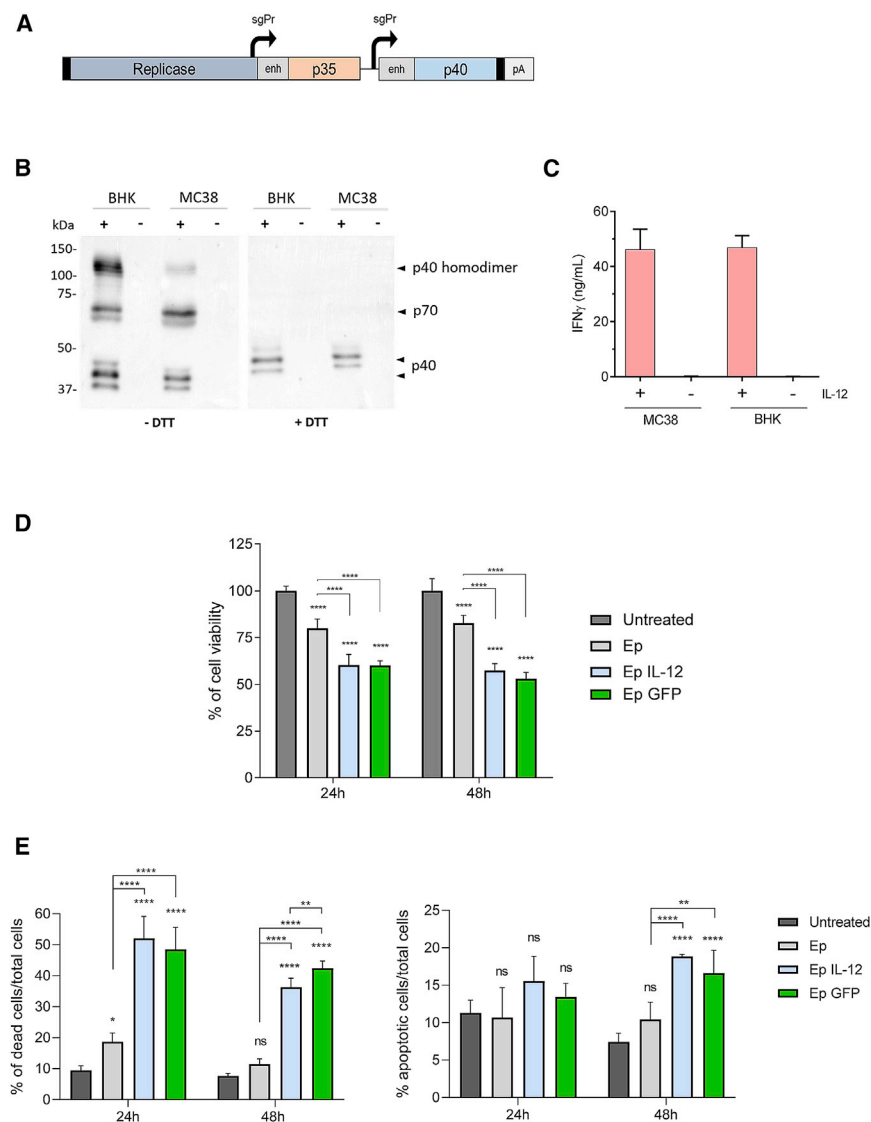


Figure 2. SFV-IL-12 saRNA electroporation *in vitro*

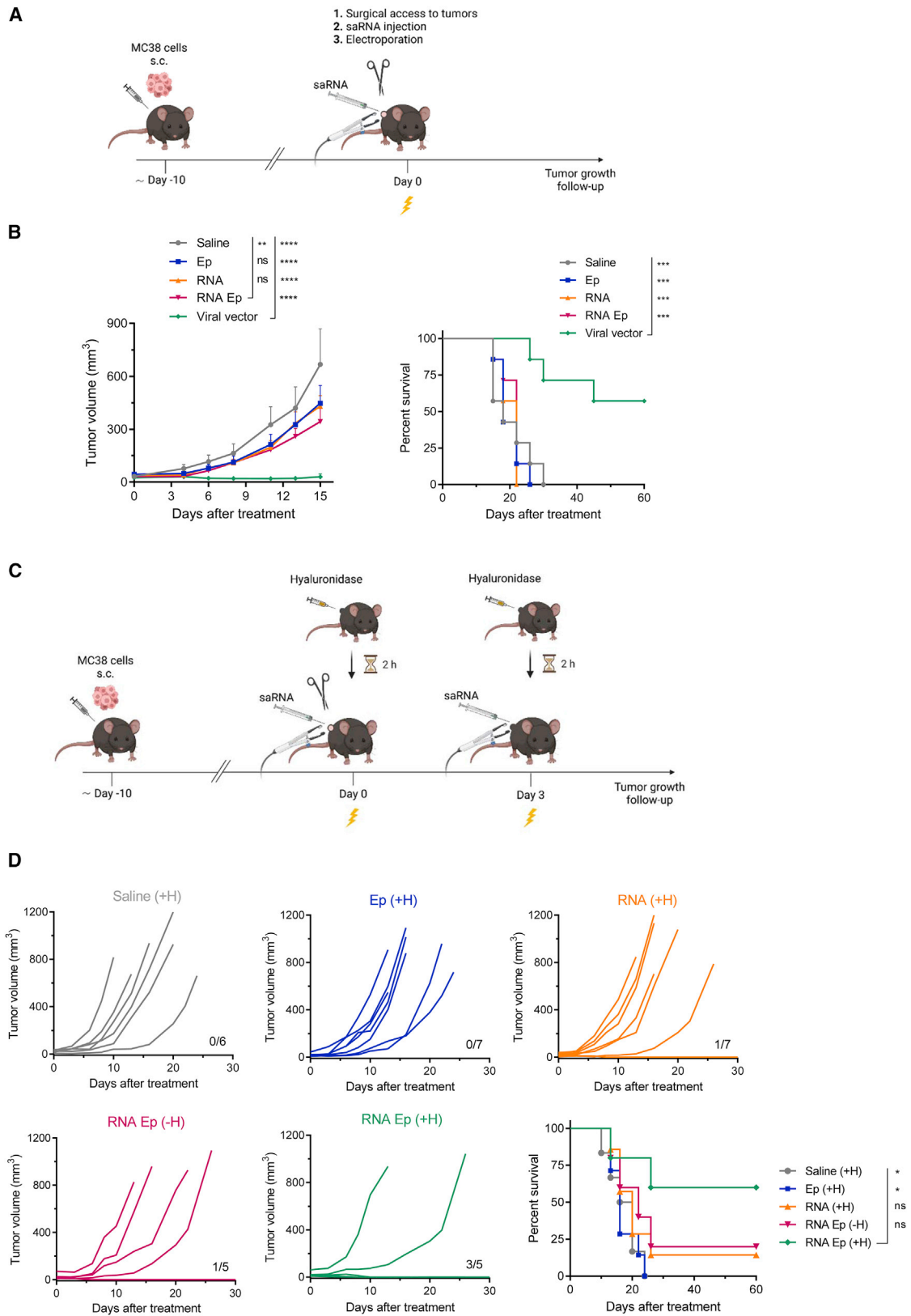
(A) Schematic representation of the SFV-IL-12 vector. (B) Western blot analysis of supernatants from MC38 and BHK-21 cells electroporated with SFV-IL-12 RNA (+) or electroporated with no RNA (-). 2×10^6 cells were electroporated with $\sim 10 \mu\text{g}$ of non-purified saRNA. Twenty-four hours later, supernatants were collected, and IL-12 was quantified by a specific ELISA. 100 ng of IL-12 was loaded onto the gel (or the equivalent volume of negative controls). The primary antibody recognizes the p40 chain of IL-12 as well as p70 (p35-p40 heterodimer) and p40 homodimer (indicated by arrows). (C) Bioactivity of IL-12 produced by electroporated cells was evaluated using mouse splenocytes. 7×10^5 mouse splenocytes were incubated with 10 ng of IL-12 produced in MC38 or BHK-21 cells or with the equivalent volume of supernatant from cells electroporated with no RNA. After 48 h, IFN- γ levels in supernatants were measured by specific ELISA. The experiment was performed with triplicate samples. Data represent mean \pm SD. sgPr, subgenomic promoter; enh, translation enhancer from the SFV capsid gene fused to the 2A self-protease from foot-and-mouth disease virus; pA, poly adenine tail; p35, IL-12 subunit p35; p40, IL-12 subunit p40; p70, IL-12 heterodimer composed of p35 and p40; DTT, dithiothreitol. (D and E) Cytotoxic effect of SFV saRNA. 3×10^6 MC38 cells were subjected to electroporation (Ep) with $\sim 40 \mu\text{g}$ of the indicated SFV saRNAs, and their viability was analyzed at the indicated times. (D) Cell viability measured by luminescence (the percentage of viable cells was calculated considering the mean of cells with no treatment as the maximum viability). (E) Cells were stained with specific markers to evaluate the percentage of dead (Zombie NIR⁺ and Annexin V⁺, left graph) and apoptotic cells (Zombie NIR⁻ and Annexin V⁺, right graph). ** $p < 0.01$; **** $p < 0.0001$.

saRNA vector, a relatively high level of Luc was still detected on day 7 after electroporation. We then compared Luc expression from SFV-Luc saRNA delivered by electroporation with that obtained when injecting tumors with a dose of 10^8 SFV-Luc viral particles (VPs), which, in previous studies, led to a strong signal in MC38 tumors.²⁵ There were no significant differences in Luc expression on days 3 and 6 between the groups (Figure 1C), indicating that saRNA delivery by electroporation could be efficient enough to generate good levels of transgene expression in MC38 tumors. Thus, the electroporation condition based on eight pulses of 0.1 ms and 1,200 V/cm was chosen for the following therapeutic experiments.

Electroporation of SFV-IL-12 saRNA in tumor cells leads to high IL-12 expression and cell death

To evaluate the therapeutic potential of local delivery of saRNA by electroporation, a SFV saRNA vector that can express high levels of

saRNA. For this experiment, we previously determined the optimal electroporation conditions using a SFV saRNA coding for GFP (SFV-GFP) and evaluated the percentage of GFP-positive cells obtained at 24 h in each case (data not shown). Then we used these conditions, described under **Materials and methods**, to electroporate SFV-IL-12 saRNA in both cell lines, and the expression of IL-12 was analyzed after 24 h in cell supernatants by ELISA and western blot. IL-12 levels obtained were around 10 and 5 $\mu\text{g}/\text{mL}$ for BHK-21 and MC38 cells, respectively. Correct dimerization of the cytokine was confirmed by western blot, where the p70 heterodimer was observed under non-reducing conditions (Figure 2B, left panel). A higher-molecular-weight band was also observed, which probably represents formation of p40 homodimers, a phenomenon that has also been described *in vivo*.³⁷ As expected, these dimers were not observed under reducing conditions (Figure 2B, right panel).



(legend on next page)

The functionality of IL-12 produced by electroporated cells was confirmed by performing an assay based on *in vitro* activation of mouse splenocytes. After 48 h of incubation with 10 ng of IL-12, supernatants from splenocytes were collected, and IFN- γ was measured by a specific ELISA as an indicator of IL-12 activity (Figure 2C). As expected, IFN- γ was only produced in splenocytes incubated with supernatants of cells electroporated with SFV-IL-12 saRNA, and similar levels of IFN- γ were produced from supernatants from both cell lines. In this experiment, we also evaluated the cytopathic effects of SFV-IL-12 saRNA in MC38 cells 24 and 48 h after electroporation, using as controls cells electroporated with SFV-GFP saRNA and without RNA as well as non-electroporated cells. As shown in Figures 2D–2E, SFV saRNA electroporation was able to significantly decrease cell viability (Figure 2D), increasing the percentages of dead and apoptotic cells (Figure 2E). This effect was much more attenuated by electroporation by itself, and no significant differences were observed between SFV-IL-12 and SFV-GFP, suggesting that RNA replication was likely the main mediator of this process, being independent of the expressed transgene.

Local electroporation of SFV-IL-12 saRNA mediates antitumor effects that can be improved by hyaluronidase treatment

To evaluate the antitumor effect of SFV-IL-12 saRNA electroporation in MC38 subcutaneous tumors, 10 μ g of saRNA was delivered *i.t.* using the electroporation conditions selected previously (eight 0.1-ms-long pulses of 1,200 V/cm and pulse interval of 0.5 s) (Figure 3A). This treatment was compared with the antitumor effect of intratumor injection of SFV-IL-12 VPs, using a dose of 10^8 VPs/tumor, which in previous studies led to a potent antitumor effect in this model.²⁵ Under these conditions, a very modest antitumor effect was observed for saRNA delivered by electroporation, in contrast to VPs, which were able to achieve more than 50% mouse survival (Figure 3B).

One of the challenges of drug delivery in solid tumors is low diffusion because of high interstitial pressure. Hyaluronan (HA) is a major component of the extracellular matrix, which is overexpressed in many tumors and could obstruct efficient delivery of medicines into the tumor microenvironment.^{38,39} Degradation of HA in the tumor stroma has been shown to enhance tumor permeability and improve the distribution of different types of medicines, including chemotherapeutic agents^{40–43} and nanoparticles,^{44,45} and, more relevant, it can increase the efficacy of gene transfection by electroporation.⁴⁶ To evaluate whether this strategy could improve the therapeutic benefit of SFV saRNA electroporation, hyaluronidase was administered *i.t.* 2 h before electroporation to promote degradation

of HA. A second saRNA electroporation was performed on day 3 to enhance and prolong *i.t.* expression of IL-12, as shown in Figure 3C. In this setting, we were able to improve the antitumor effect of SFV-IL-12 saRNA electroporation, leading to 60% complete regression, which was reflected in similar long-term survival of the animals (Figure 3D). Although inclusion of a second saRNA electroporation slightly improved the antitumor effect, leading to 20% complete remission, injection of hyaluronidase seemed to be important for an optimal antitumor effect. These results were reproduced in a second tumor model based on hepatocellular carcinoma (HCC) PM299L cells implanted subcutaneously into mice. In this case, electroporation of SFV-IL-12 saRNA, using the optimal conditions used for MC38 tumors, led to a significant reduction of PM299L tumor growth and 88% of complete regression with long-term survival (Figure 4).

IL-12 saRNA electroporation induces antitumor cellular immune responses

To elucidate some of the mechanisms implicated in the antitumor effect of SFV-IL-12 saRNA electroporation, mice bearing larger MC38 tumors (~5 mm in diameter) were treated according to the protocol described in Figure 3C. Six days after the second round of electroporation, they were sacrificed to evaluate the induced antitumor immune response. SFV-IL-12 saRNA electroporation led to a significant decrease in tumor growth compared with untreated mice and with both single therapies (Figure 5A). In fact, two of five mice in this group presented complete remission at sacrifice despite the larger initial tumor size. Tumor weights at sacrifice were also lower for all animals treated with saRNA plus electroporation compared with the single therapies, confirming the potency of this strategy in larger tumors (Figure 5B). Splenocytes were collected and co-cultured with irradiated MC38 cells at a 10:1 lymphocyte:tumor cell ratio to measure the IFN γ -producing lymphocytes by ELISPOT. As shown in Figure 5C, mice electroporated *i.t.* with SFV-IL-12 saRNA produced a significantly higher number of IFN γ -secreting cells in comparison with mice that received only saRNA or electroporation. In mice with PM299L tumors that were cured after SFV-IL-12 saRNA electroporation, we also observed higher numbers of IFN-gamma producing cells after stimulation with tumor cells (PM299L) or SIINFEKL peptide (PM299L cells express this peptide) compared with naive mice (Figure S1). This experiment was performed 55 days after the second electroporation, indicating that, in this model, a strong memory immune response had also been induced.

Tumor-infiltrating lymphocytes (TILs) were collected to carry out an immunophenotypic analysis by flow cytometry. According to the

Figure 3. Antitumor efficacy of SFV-IL-12 saRNA Ep in MC38 tumors

Mice bearing ~30-mm³ MC38 subcutaneous tumors were treated *i.t.* with 10 μ g of SFV-IL-12 saRNA plus Ep (RNA Ep) or the single treatments as controls (Ep or RNA alone). (A) Schematic of the Ep protocol used in (B). (B) Antitumor activity of SFV-IL-12 saRNA Ep compared with administration of SFV-IL-12 VPs (10^8 VP/tumor). Data represent the mean tumor volume (mm³) \pm SEM (left) and survival proportions (right). (C and D) Effect of local hyaluronidase treatment on the antitumor activity of SFV-IL-12 saRNA Ep. (C) Schematic of the optimized protocol for SFV saRNA *i.t.* Ep used in (D). Two rounds of treatment were performed on days 0 and 3. Hyaluronidase was administered *i.t.* 2 h before each procedure (30 units/tumor). (D) Data represent individual tumor volumes for mice of each group (mm³) and survival proportions (bottom right panel). All animals received hyaluronidase (+H) except one control group (–H). The fractions in the bottom right corner of the tumor size graphs indicate the number of complete regressions/total number of mice in each group. * $p < 0.05$, ** $p < 0.01$, *** $p < 0.001$, **** $p < 0.0001$.

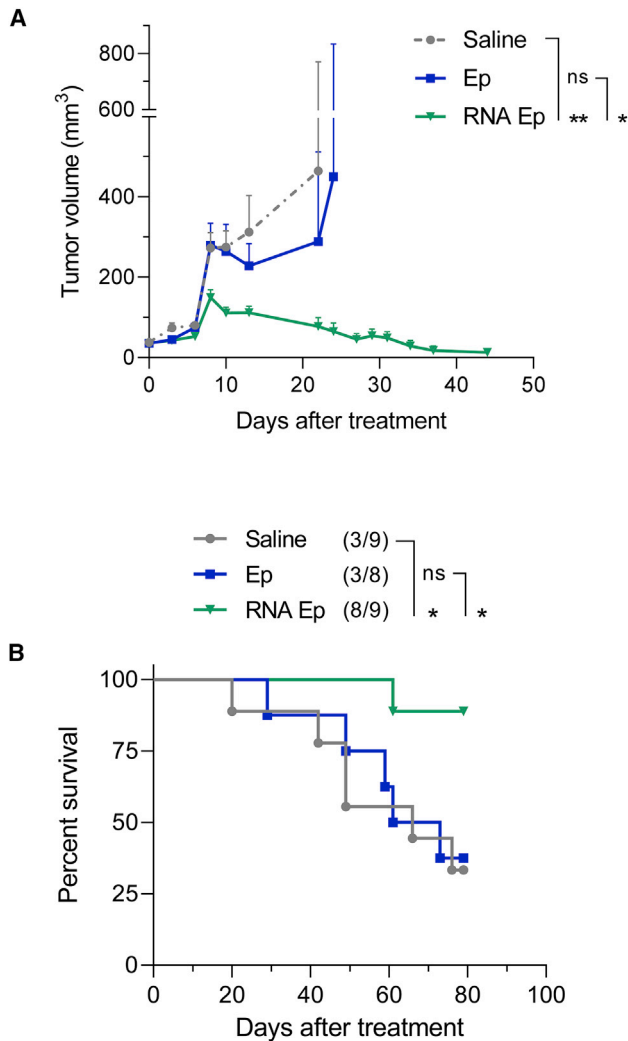


Figure 4. Antitumor efficacy of SFV-IL-12 saRNA Ep in PM299L tumors
Mice bearing $\sim 35 \text{ mm}^3$ PM299L subcutaneous tumors were treated i.t. with $10 \mu\text{g}$ of SFV-IL-12 saRNA plus electroporation (RNA Ep, $n = 9$), only Ep (Ep, $n = 8$), or saline without Ep (saline, $n = 9$) as described in Figure 3C. (A) Average tumor growth along time. Data represent the mean tumor volume (mm^3) \pm SEM. Statistical comparisons were done on day 20 when all mice were still alive. (B) Survival proportions. The fractions to the left of group names indicate the number of complete regressions/total number of mice in each group. * $p < 0.05$, ** $p < 0.01$.

antitumor effect shown in Figures 5A and 3D, we found that mice treated with electroporation with SFV-IL-12 saRNA had a trend to have a higher number of CD8^+ T cells (Figure 5D, top left graph). This combination group showed significantly higher numbers of CD8^+ T cells expressing the activation markers PD-1 and ICOS (Figure 5D, center and right panels, respectively) and proliferating (Ki67^+) CD8^+ T cells expressing the activation marker granzyme B (Figure 5E). These mice also had a higher percentage of tumor-specific (MuLV tetramer^+) CD8^+ T cells (Figure 5F, left graph) in which ICOS was upregulated (Figure 5F, right graph). Finally, the CD4^+

CD8^+ ratio was significantly lower in the combination group in comparison with electroporation or saRNA administration monotherapy (Figure 5G, left graph). CD4^+ T cells also showed higher PD-1 expression in mice electroporated with saRNA (Figure 5G, right graph).

An additional mechanism involved in tumor regression could be induction of cancer cell death because of RNA replication or the electroporation process. To evaluate this possibility, we analyzed the presence of necrotic areas in MC38 tumors 5 days after the different treatments. As shown in Figure S2, necrotic areas were only observed in tumors electroporated with or without RNA, although the effect was more evident in the last case, suggesting that RNA replication and electroporation could be contributing to cancer cell death.

As a conclusion, the intratumor *in vivo* electroporation of a saRNA encoding IL-12 is able to control tumor growth, promote a higher percentage of $\text{IFN}\gamma$ -producing lymphocytes, and lead to an increase in the percentages of active and cytotoxic CD8^+ TILs in comparison with mice treated with electroporation or saRNA alone.

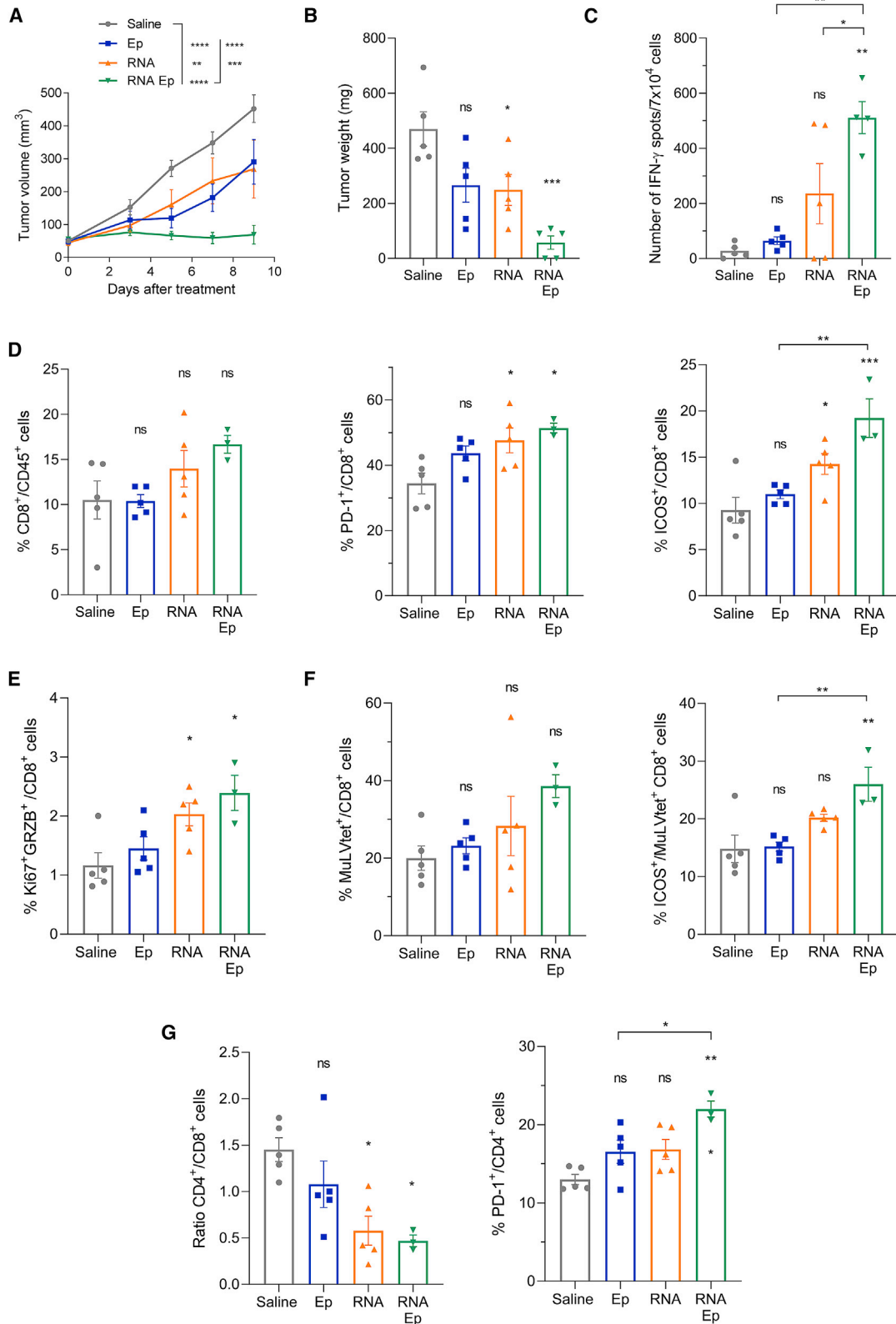
Combination of IL-12 saRNA electroporation and PD-1 blockade can enhance the antitumor effect

Combination of the SFV viral vector encoding for IL-12 and PD-1/PD-L1 blockade has been shown to work synergistically, probably because of upregulation of PD-L1 expression in tumor cells via $\text{IFN}\gamma$.⁴⁷ We hypothesized that combination of intratumor IL-12 saRNA electroporation and PD-1 blockade could result in a more potent antitumor effect as well. To evaluate this, mice bearing MC38 subcutaneous tumors were treated with SFV-IL-12 saRNA plus electroporation, as described before, in combination with systemic anti-PD-1 antibody. Mice treated with this strategy showed a remarkable effect on controlling tumor growth, leading to 80% complete regression and long-term survival (Figures 6A and 6B). This effect was superior compared with animals that received SFV-IL-12 saRNA plus electroporation without anti-PD-1, although this treatment also had a potent antitumor effect, as observed in earlier experiments (Figures 3D, 5A, and 5B). Control groups based on electroporation or saRNA also showed some degree of tumor growth delay, especially the one including combination of electroporation plus systemic anti-PD-1 antibody treatment. However, none of these treatments were able to significantly increase the survival of the animals compared with the untreated group.

Animals that rejected the tumors were rechallenged with the same tumor cell line 3 months later. All animals showed protection from this rechallenge, suggesting induction of the memory antitumor immune response (Figure 6C).

DISCUSSION

Use of RNA for vaccination has become a reality with the recent development of coronavirus disease 2019 (COVID-19) vaccines, which have proven to be very efficient to prevent severe acute respiratory syndrome coronavirus 2 (SARS-CoV-2) infection.⁴⁸ Although these vaccines are based on mRNA, some prototypes have also been



(legend on next page)

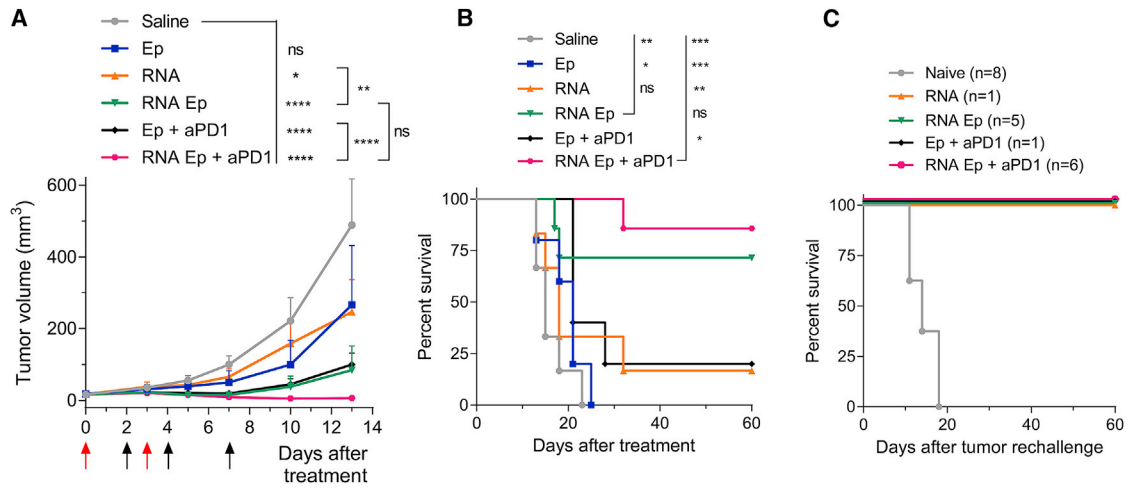


Figure 6. SFV-IL-12 saRNA plus Ep and systemic PD-1 blockade can enhance the antitumor effect

Mice underwent two rounds of RNA Ep on days 0 and 3 (red arrows) with hyaluronidase pretreatment, as described in Figure 3C. A systemic anti-PD-1 antibody was administered on days 2, 4, and 7 (black arrows) in combination with RNA Ep (RNA Ep + aPD1). Control groups received SFV-IL-12 saRNA alone (RNA), electroporation (Ep), or Ep plus anti-PD-1 treatment (Ep + aPD1) or were left untreated (saline). (A) Tumor size progression. Data represent the mean tumor volume (mm^3) \pm SEM. (B) Survival proportions. (C) Survival proportions after tumor rechallenge. Mice with complete remissions were rechallenged with 5×10^5 MC38 cells after 3 months. Naive untreated mice were used as controls. * $p < 0.05$, ** $p < 0.01$, *** $p < 0.001$, **** $p < 0.0001$.

developed based on saRNA, which in preclinical studies have shown to elicit similar immune responses but at much lower doses.^{49,50} This is probably due to the fact that saRNA can not only express higher antigen levels, but it can also elicit IFN type I responses and apoptosis, enhancing immune responses and allowing release of the expressed antigens, respectively.⁵¹ These properties of saRNA can also be exploited to induce antitumor responses by expression of tumor antigens or immunostimulatory molecules. This approach has been used previously by us and others to deliver into tumors VPs containing saRNA expressing cytokines and immunomodulatory antibodies, which were able to induce potent antitumor responses in several tumor models.^{28,52} A recent clinical trial has shown that vaccination with SFV VPs expressing the human papillomavirus proteins E6 and E7 was able to induce cellular immune responses in individuals with cervical intraepithelial neoplasia.⁵³ However, use of VPs has some drawbacks that could limit their clinical translation, such as biosafety issues and difficulties to produce them at GMP levels. For that reason, in the present study, we explored the possibility of using naked saRNA for local delivery of IL-12 to tumors. To enhance entry of the saRNA into tumor cells, we employed *in vivo* electroporation, a technique that can induce formation of pores in cell membranes,

facilitating RNA entry. Electroporation by itself could also induce antitumor effects, especially when a high voltage is used. In fact, irreversible electroporation (IRE), which induces a high proportion of cell death in the pulsed area, is currently used in the clinic as a tumor ablation technique for some accessible tumors.⁵⁴ We have shown previously that the antitumor effects of IRE can be potentiated by combining it with adjuvants able to promote type I IFN responses, such as poly(IC:LC) (polyinosinic-polycytidylic acid and poly-L-lysine, a dsRNA analog mimicking viral RNA) or STING agonists.^{11,12} Based on these results, we reasoned that combination of electroporation with an saRNA expressing a potent immunostimulatory cytokine, such as IL-12, could further improve the antitumor effects of this technique. We first optimized electroporation conditions using a saRNA expressing Luc as a reporter gene. Previous reports have shown that saRNA could be optimally electroporated in the skin of mice by applying a couple of short high-voltage pulses followed by eight long low-voltage pulses.^{33,35} The rationale for this strategy was that the initial high-voltage pulses could create multiple pores in cell membranes, whereas the following string of low-voltage pulses would help move the RNA inside the cells. However, in contrast to these results, we observed higher transfection and

Figure 5. SFV-IL-12 saRNA Ep induces antitumor immune responses

Mice bearing $\sim 50 \text{ mm}^3$ MC38 subcutaneous tumors were injected i.t. with hyaluronidase 2 h before the indicated treatments: Ep alone (Ep), SFV-IL-12 saRNA without electroporation (RNA), or SFV-IL-12 saRNA plus electroporation (RNA Ep) on days 0 and 3, according to the protocol schematized in Figure 3C. The control group received hyaluronidase and saline solution (saline). Nine days after the beginning of the treatment, mice were sacrificed, and tumors and spleens were collected for analysis. (A) Tumor size progression. Data represent the mean tumor volume (mm^3) \pm SEM. (B) Tumor weights at sacrifice (day 9). (C) IFN γ -producing cell numbers measured by ELISPOT assay. The graph represents IFN γ -producing cells/ 0.7×10^6 T cells. (D–G) Immunophenotypic characterization of tumor-infiltrating lymphocytes (TILs). (D and E) Analysis of CD8 $^+$ TILs with the indicated markers. (F) Analysis of MuLV-specific tetramer $^+$ CD8 $^+$ T cells with the indicated markers. (G) Analysis of CD4 $^+$ /CD8 $^+$ ratio (left) and CD4 $^+$ TILs expressing PD-1 (right). Asterisks above bars indicate statistical comparison of each group with the control saline group. Other comparisons are indicated with horizontal bars. * $p < 0.05$, ** $p < 0.01$, *** $p < 0.001$, **** $p < 0.0001$.

reproducibility when applying eight short high-voltage pulses. These conditions led to a level of Luc expression that was not significantly different than the one obtained by injecting the tumor with 10^8 VPs of SFV-Luc, indicating that electroporation and infection with VPs could achieve comparable tumor transduction. A certain degree of variability in Luc expression was observed in these experiments, which could be due to RNA degradation. This happened despite the fact that RNase inhibitors were added to the RNA during synthesis and before tumor injection, something that has allowed better repeatability of results in previous studies using a saRNA electroporated intradermally in mice.³⁶

By using our optimal electroporation conditions with SFV-IL-12 RNA, we were able to induce a significant antitumor effect in MC38 colon adenocarcinoma and PM299L HCC tumors. This effect was highly potentiated by injecting tumors with hyaluronidase before electroporation. This enzyme can degrade the HA-rich matrix present in the tumor, probably allowing better distribution of the saRNA, which, after electroporation, could have access to a higher number of cells. Enhancement of tumor-targeting and antitumor effects using hyaluronidase has been observed previously in studies using oncolytic viruses⁵⁵ or plasmid electroporation.⁴⁶ In this last case, the best results were obtained by combining hyaluronidase and collagenase, something that could be tested in future research with saRNA electroporation. Although use of hyaluronidase might limit clinical use of this strategy, this compound has already been approved for clinical use,⁵⁶ and its injection in tumors not located on the body surface could be done by ultrasound-guided percutaneous access.

In our studies, electroporation by itself or injection of naked saRNA without electroporation only showed marginal antitumor effects, indicating that a combination of the two strategies is needed for optimal results. As observed in a previous study performed with SFV-IL-12 VP,²⁸ the antitumor effect obtained after SFV-IL-12 RNA electroporation seemed to be mediated mainly by CD8⁺ T cells because a significant increase in activation markers, such as PD-1, ICOS, and granzyme, was observed in CD8⁺ TILs from mice receiving saRNA and electroporation. A specific antitumor response was only observed in this group, as indicated by the higher i.t. CD8⁺ cells able to recognize MC38 MuLV tumor-specific antigen or by specific ELISPOT, in which splenocytes are stimulated with tumor cells. The fact that PD-1 expression was higher in CD8⁺ and CD4⁺ TILs of the combination group indicated that these cells were more active but that they could also be blocked by PD-L1 expressed by tumor cells. In fact, we and others have observed previously that MC38 tumors can express PD-L1,^{52,57} something that could dampen the antitumor responses. Accordingly, combination of SFV-IL-12 electroporation with an anti-PD-1 monoclonal antibody (mAb) was able to further potentiate the therapeutic effect of this therapy. Because we have shown earlier that intratumor delivery of SFV VP expressing anti-PD-L1 (SFV-aPD-L1) can induce potent antitumor effects,⁵² in future experiments it would be interesting to test whether electroporation of SFV-aPD-L1 RNA can also lead to therapeutic efficacy. In this regard, saRNAs expressing IL-12 and an anti-PD-L1 mAb could be admixed prior to electroporation

to obtain optimal results. Alternatively, the saRNA could be engineered to express both molecules, something that would be harder to achieve when using the vector as VPs because of the packaging constrictions of the viral capsid. An additional advantage of saRNA electroporation over VP is the fact that no anti-vector immune response will be generated, something that, in the latter case, could prevent re-administration of the vector or diminish the effect of subsequent doses.⁵⁸ Our results suggest that delivery of saRNA by electroporation could be an attractive strategy for local cancer immunotherapy. This approach could have easier translation to clinical practice, especially for percutaneously accessible tumors.

MATERIALS AND METHODS

Cell lines and animals

BHK-21 cells (ATCC-CCL10) were cultured in GMEM-BHK21 (Thermo Fisher Scientific, Waltham, MA) supplemented with 5% fetal bovine serum (FBS), 10% tryptose phosphate broth, 2 mM glutamine, 20 mM HEPES, and antibiotics (100 µg/mL streptomycin and 100 U/mL penicillin). MC38 cells, a kind gift from Dr. Karl E. Hellström (University of Washington, Seattle, WA), and PM-299L cells (provided by Dr. Amaia Lujambio, Icahn School of Medicine at Mount Sinai, New York, NY) were cultured in RPMI-1640 medium (Lonza, Switzerland) supplemented with 10% FBS, 2 mM glutamine, 20 mM HEPES, antibiotics, and 50 µM 2-mercaptoethanol (RPMI-1640 complete medium).

Six-week-old female C57BL/6J mice were purchased from Envigo (Barcelona, Spain). Animal studies were approved by the Universidad de Navarra ethical committee (study 018-19) for animal experimentation under Spanish regulations.

RNA synthesis and production of viral vectors

SFV plasmids coding for firefly Luc (pSFV-Luc) or mouse IL-12 with a translation enhancer (pSFV-enhIL12) have been described previously²⁵ and were used to synthesize SFV-Luc and SFV-IL-12 saRNAs, respectively. pSFV-GFP, used to synthesize SFV-GFP saRNA, was kindly provided by Prof. P. Liljeström (Karolinska Institute, Sweden). *In vitro* transcription of RNA from these plasmids was performed as described previously.⁵⁹ Briefly, SFV plasmids linearized with Spe I were used as templates to synthesize RNA using SP6 RNA polymerase (Promega, Madison, WI) for 1 h at 37°C in 50- to 150 µL reaction mixtures containing the m⁷G(5')ppp(5')G RNA cap structure analog (New England Biolabs, Ipswich, MA). For *in vitro* experiments, RNA was used immediately after transcription or stored at -80°C until use. For *in vivo* studies, RNA was precipitated using 0.5 M LiCl for 1 h at -20°C and subsequent centrifugation at 13,000 × g for 30 min at 4°C. The RNA pellet was washed with 70% ethanol and centrifuged under the same conditions for 20 min. After drying the RNA pellet at room temperature for 5–10 min, it was resuspended with diethyl pyrocarbonate (DEPC)-treated sterile H₂O to a final concentration of approximately 1 µg/µL, its integrity was checked by gel electrophoresis and its concentration measured by Nanodrop spectrophotometer. Aliquots were stored at -80°C. DEPC-treated PBS and RNasin Plus RNase inhibitor (Promega) were added before electroporation.

Packaging of recombinant saRNA into SFV VPs was performed by co-transfecting BHK-21 cells by electroporation with equal amounts of three RNAs: recombinant saRNA encoding the transgene of interest and two helper RNAs (SFV-helper-C-S219A and SFV-helper-S2 RNAs) that provide the SFV capsid and envelope proteins in *trans*, respectively.⁶⁰ After electroporation, cells were cultured for 4 h at 37°C and then for 48 h at 33°C and 5% CO₂. VPs were purified by ultracentrifugation and titrated by infection of BHK-21 cells with serial dilutions of the VP stocks as described previously.⁶¹ Indirect immunofluorescence was performed 24 h later using an in-house produced rabbit polyclonal antiserum that recognizes the nsp2 subunit of SFV replicase.

Analysis of *in vitro* expression of IL-12

2×10^6 MC38 or BHK-21 cells were electroporated with $\sim 10 \mu\text{g}$ of *in-vitro*-transcribed SFV-IL-12 saRNA in 400 μL (MC38) or 800 μL (BHK-21) of PBS using 4-mm electroporation cuvettes and the Gene Pulser II electroporator (Bio-Rad, Hercules, CA). The electroporation parameters for MC38 cells (1 pulse of 500 V, 25 μF) were optimized using SFV-GFP saRNA, and parameters for BHK-21 cells (2 pulses of 850 V, 25 μF) have been described previously.⁵⁹ Electroporated cells were cultured for 24 h at 37°C and 5% CO₂, and then supernatants were collected to analyze IL-12 secretion. Quantification of IL-12 was performed by a commercial specific ELISA (BD Biosciences, Franklin Lakes, NJ). Western blot analysis was carried out using a rat antibody that recognizes the p40 subunit of mouse IL-12 (BD Biosciences). To verify IL-12 bioactivity, 10^6 mouse splenocytes/well were incubated in U-bottom 96-well plates with 10 ng of IL-12 in RPMI-1640 complete medium for 48 h at 37°C and 5% CO₂. Then supernatants were collected, and IFN- γ secretion was quantified using a commercial specific ELISA (BD Biosciences).

Cytotoxic effect of saRNA *in vitro*

3×10^6 MC38 cells and 40 μg of saRNA were mixed in 400 μL of PBS and electroporated as described before. Cells were recovered in complete RPMI-1640 medium, and 10,000 cells were seeded in 96-well white or transparent plates. Cell viability was measured from white plates 24 and 48 h after electroporation using the CellTiter Glo kit (Promega), following the manufacturer's instructions. Luminescence was measured on a GloMax luminometer (Promega). For flow cytometry analysis, cells were stained with Zombie NIR viability dye (BioLegend, San Diego, CA) and phycoerythrin (PE) Annexin V, following the manufacturer's instructions. Samples were acquired on a FACSCanto-II cytometer (BD Biosciences). Data were analyzed using FlowJo software (Tree Star, Ashland, OR).

Tumor induction and treatment

Mice were injected subcutaneously (s.c.) with 5×10^5 MC38 or PM-299L cells diluted in 50 μL of saline in the right flank. For all electroporation experiments, 10 μg /tumor of SFV saRNA in a maximum volume of 20 μL was used. Pulses were delivered using the ECM 830 electroporation system (BTX, Holliston, MA) and tweezer electrodes (1 mm, BTX).

For Luc expression experiments, tumors with a medium size of 5 mm in diameter were electroporated once using the electroporation conditions detailed in Figure 1. By making a small superficial incision in the skin close to the tumor location, we first exposed the tumors to avoid possible interference of the skin during pulse delivery. After that, the RNA was injected i.t. with a Hamilton syringe, and electroporation was performed. Incisions were closed using clamps for 2–3 days. For this procedure, mice were anesthetized with 40 μL of a mixture of ketamine, physiological saline, and xylazine (at a ratio of 9:9:2) administered intraperitoneally (i.p.), and a single dose of 5 mg/kg of ketoprofen was administered s.c. to prevent any discomfort.

For therapeutic experiments, the treatment schedule started approximately 10 days after tumor inoculation, when tumors reached a medium size of 3–4 mm in diameter. The optimized treatment consisted of a 3-day regimen for which mice underwent two rounds of electroporation. The first electroporation was carried out as described before, and the second one was performed without the surgical procedure. Hyaluronidase type IV-S (Sigma, St. Louis, MO) was administered i.t. 2 h before each electroporation (30 units/tumor in 25 μL of PBS).

For systemic PD-1 blockade, an anti-PD-1 antibody RMPI-14 clone (Bio X Cell, Lebanon, NH) was administered i.p. on days 2, 4, and 7 (100 μg /mice for each dose).

Efficacy of treatments was evaluated by measuring two perpendicular tumor diameters every 2–3 days, and tumor volumes (mm^3) were calculated using the formula $\text{volume} = (\text{length} \times \text{width}^2)/2$. Mice were sacrificed when tumors reached a size of approximately 1,200 mm^3 or when pain or tumor ulceration was observed.

For histological analysis of treated MC38 tumors, mice were sacrificed 5 days after the second round of treatment, and tumors were collected. Formalin-fixed, paraffin-embedded sections (3 μm thick) were stained with hematoxylin and eosin.

Bioluminescence imaging of mice

For *in vivo* quantification of Luc activity, mice were anesthetized as described before and received 100 μL i.p. of a 30 $\mu\text{g}/\text{mL}$ solution of D-luciferin potassium salt substrate (Promega) dissolved in PBS. Light emission was measured 10 min after substrate administration using a CCD luminometric camera (Biospace Lab, France). Image processing and signal intensity quantifications were performed using M3 Vision software (Biospace Lab). The number of photons emitted per square centimeter per second per steradian ($\text{ph}/\text{s}/\text{cm}^2/\text{sr}$) was used as a measure of Luc activity.

Flow cytometry

For immunophenotypic characterization of T cells, spleens and tumors were collected from each mouse 6 days after the second round of treatment. Excised tumors were digested with 400 U/mL collagenase D and 50 $\mu\text{g}/\text{mL}$ DNase-I (Roche, Switzerland) for 20 min at 37°C. After washing with PBS, red cells were lysed with ACK buffer (Sigma). Spleens were homogenized in PBS using a 70- μm filter.

For functional analyses, cells were incubated with Zombie NIR viability dye (BioLegend). Then, to identify tumor-specific CD8⁺ T lymphocytes, we stained cells with H-2Kb MuLV p15E Tetramer-KSPWF^TTL (MBL International, Woburn, MA). Subsequently, they were stained with fluorochrome-conjugated mAbs against CD45.2 (clone 104), CD8 (clone 53.6.7), CD4 (clone RM4-5), ICOS (clone 7E.17G9) (all of them from BioLegend), and PD-1 (clone RMP1-30, Invitrogen). For intracellular staining, cells were fixed and permeabilized with BD Fixation/Perm buffer (BD Biosciences) and then stained with anti-granzyme B (clone GB11, BioLegend) and anti-Ki67 (clone 16A8, Invitrogen) mAbs. Samples were acquired on a FACSCanto-II cytometer (BD Biosciences). Data were analyzed using FlowJo software (Tree Star). Gating strategies are shown in [Figure S3](#).

ELISPOT

Following the instructions of a commercial IFN γ ELISPOT kit (BD Biosciences), the number of IFN γ -producing cells was analyzed in collected splenocytes. Briefly, a 96-well plate was coated the day before the assay with an anti-mouse IFN γ capture antibody at a concentration of 5 μ g/mL in PBS. After overnight incubation at 4°C, the antibody was discarded, and the plate was blocked with RPMI-1640 complete medium for 2 h at room temperature (RT). Splenocytes (7×10^5 /well) were co-cultured with irradiated MC38 or PM299L cells (using 14,000 cGy) at a 10:1 lymphocyte:tumor cell ratio or with SIINFEKL peptide. After 1 day of co-culture, the number of IFN γ ⁺ spot-forming cells was revealed by a colorimetric reaction, and spots were counted with an automated ELISPOT reader (CTL, Aalen, Germany).

Statistical analysis

All data are expressed as the mean \pm SEM unless otherwise specified. Prism software (GraphPad, San Diego, CA) was used for statistical analysis. To compare multiple experimental groups, one-way ANOVA test and Tukey's multiple comparison test were used. In [Figures 1B, 1C, 4A, and S1](#), comparisons between different groups were performed using a Mann-Whitney test. For time-series analysis, data were compared using the extra sum-of-squares F test and fitted to a second-order polynomial equation. Survival of tumor-bearing mice is represented by Kaplan-Meier plots and analyzed by log-rank test. $p < 0.05$ was considered statistically significant.

DATA AVAILABILITY

The data supporting the findings of this study are available within the manuscript or in the [supplemental information](#) or available from the corresponding author upon request.

SUPPLEMENTAL INFORMATION

Supplemental information can be found online at <https://doi.org/10.1016/j.omtn.2022.07.020>.

ACKNOWLEDGMENTS

We would like to thank the personnel at the Cima Universidad de Navarra animal facility for excellent help. This research was funded

by Fundación Bancaria La Caixa (project reference: CIMA TRANSFIERE CAIXA SIRENA), Ministerio de Ciencia e Innovación (PID2019-108989RB-I00), Instituto Salud Carlos III financed with Feder Funds PI17/01859 and PI20/00415 (“A way to make Europe”) and CARPanTu PLEC2021-008094 MCIN/AEI/10.13039/501100011033/European Union NextGenerationEU/PRTR, Gobierno de Navarra Industria (0011-1411-2019-000079, Proyecto DESCARTheS and 0011-1411-2022-000088; Proyecto SOCRATheS), and Gobierno de Navarra Departamento de Salud 64/2019 (co-financed at 50% by the European Regional Development Fund through the FEDER Operational Program 2014–2020 of Navarra: “European Union. European Regional Development Fund. A way to make Europe”). N.S.-P. has the fellowship “Ayudas predoctorales de investigación biomédica AC.” A.L.-C. has the fellowship “Gobierno de Navarra, ayudas predoctorales.”

AUTHOR CONTRIBUTIONS

Conceptualization, supervision, project administration, and funding acquisition, J.J.L. and C.S.; methodology, N.S.-P., A.L.-C., C.M.-O., and T.L.; investigation, N.S.-P., A.L.-C., C.M.-O., and T.L.; formal analysis, A.L.-C., N.S.-P., and T.L.; resources, J.J.L. and C.S.; writing – original draft, N.S.-P., A.L.-C., J.J.L., and C.S.; writing – review & editing, J.J.L., C.S., N.S.-P., and A.L.-C. All authors have read and agreed to the published version of the manuscript.

DECLARATION OF INTERESTS

The authors declare no competing interests.

REFERENCES

- Waldman, A.D., Fritz, J.M., and Lenardo, M.J. (2020). A guide to cancer immunotherapy: from T cell basic science to clinical practice. *Nat. Rev. Immunol.* *20*, 651–668.
- Pai, S.I., Cesano, A., and Marincola, F.M. (2020). The paradox of cancer immune exclusion: immune oncology next frontier. *Cancer Treat Res.* *180*, 173–195.
- Demaria, S., and Formenti, S.C. (2020). The abscopal effect 67 years later: from a side story to center stage. *Br. J. Radiol.* *93*, 20200042.
- Livraghi, T., Meloni, F., Di Stasi, M., Rolle, E., Solbiati, L., Tinelli, C., and Rossi, S. (2008). Sustained complete response and complications rates after radiofrequency ablation of very early hepatocellular carcinoma in cirrhosis: is resection still the treatment of choice? *Hepatology* *47*, 82–89.
- Facciorusso, A., Abd El Aziz, M.A., Tartaglia, N., Ramai, D., Mohan, B.P., Cotsoglou, C., Pusceddu, S., Giacomelli, L., Ambrosi, A., and Sacco, R. (2020). Microwave ablation versus radiofrequency ablation for treatment of hepatocellular carcinoma: a meta-analysis of randomized controlled trials. *Cancers* *12*, 3796.
- Rangamuwa, K., Leong, T., Weeden, C., Asselin-Labat, M.-L., Bozinovski, S., Christie, M., John, T., Antippa, P., Irving, L., and Steinfurt, D. (2021). Thermal ablation in non-small cell lung cancer: a review of treatment modalities and the evidence for combination with immune checkpoint inhibitors. *Transl. Lung Cancer Res.* *10*, 2842–2857.
- Sangro, B., Iñárraiegui, M., and Bilbao, J.I. (2012). Radioembolization for hepatocellular carcinoma. *J. Hepatol.* *56*, 464–473.
- Philips, P., Hays, D., and Martin, R.C.G. (2013). Irreversible electroporation ablation (IRE) of unresectable soft tissue tumors: learning curve evaluation in the first 150 patients treated. *PLoS One* *8*, e76260.
- Narayanan, J.S.S., Ray, P., Hayashi, T., Whisenant, T.C., Vicente, D., Carson, D.A., Miller, A.M., Schoenberger, S.P., and White, R.R. (2019). Irreversible electroporation combined with checkpoint blockade and TLR7 stimulation induces antitumor immunity in a murine pancreatic cancer model. *Cancer Immunol. Res.* *7*, 1714–1726.

10. Rodríguez-Ruiz, M.E., Perez-Gracia, J.L., Rodríguez, I., Alfaro, C., Oñate, C., Pérez, G., Gil-Bazo, I., Benito, A., Inogés, S., López-Díaz de Cerio, A., et al. (2018). Combined immunotherapy encompassing intratumoral poly-ICLC, dendritic-cell vaccination and radiotherapy in advanced cancer patients. *Ann. Oncol.* *29*, 1312–1319.
11. Vivas, I., Iribarren, K., Lozano, T., Cano, D., Lasarte-Cia, A., Chocarro, S., Gorraiz, M., Sarobe, P., Hervás-Stubbs, S., Bilbao, J.I., et al. (2019). Therapeutic effect of irreversible electroporation in combination with poly-ICLC adjuvant in preclinical models of hepatocellular carcinoma. *J. Vasc. Interv. Radiol.* *30*, 1098–1105.
12. Lasarte-Cia, A., Lozano, T., Cano, D., Martín-Otal, C., Navarro, F., Gorraiz, M., Casares, N., Vivas, I., and Lasarte, J.J. (2021). Intratumoral STING agonist injection combined with irreversible electroporation delays tumor growth in a model of hepatocarcinoma. *BioMed Res. Int.* *2021*, 8852233.
13. Yang, Z.x., Wang, D., Wang, G., Zhang, Q.h., Liu, J.m., Peng, P., and Liu, X.h. (2010). Clinical study of recombinant adenovirus-p53 combined with fractionated stereotactic radiotherapy for hepatocellular carcinoma. *J. Cancer Res. Clin. Oncol.* *136*, 625–630.
14. Friedman, G.K., Johnston, J.M., Bag, A.K., Bernstock, J.D., Li, R., Aban, I., Kachurak, K., Nan, L., Kang, K.-D., Totsch, S., et al. (2021). Oncolytic HSV-1 G207 immunovirotherapy for pediatric high-grade gliomas. *N. Engl. J. Med.* *384*, 1613–1622.
15. Kim, W., Seong, J., Oh, H.J., Koom, W.S., Choi, K.-J., and Yun, C.-O. (2011). A novel combination treatment of armed oncolytic adenovirus expressing IL-12 and GM-CSF with radiotherapy in murine hepatocarcinoma. *J. Radiat. Res.* *52*, 646–654.
16. Trinchieri, G. (2003). Interleukin-12 and the regulation of innate resistance and adaptive immunity. *Nat. Rev. Immunol.* *3*, 133–146.
17. Voest, E.E., Kenyon, B.M., O'Reilly, M.S., Truitt, G., D'Amato, R.J., and Folkman, J. (1995). Inhibition of angiogenesis in vivo by interleukin 12. *J. Natl. Cancer Inst.* *87*, 581–586.
18. Mazzolini, G., Narvaiza, I., Pérez-Diez, A., Rodríguez-Calvillo, M., Qian, C., Sangro, B., Ruiz, J., Prieto, J., and Melero, I. (2001). Genetic heterogeneity in the toxicity to systemic adenoviral gene transfer of interleukin-12. *Gene Ther.* *8*, 259–267.
19. Nguyen, K.G., Vrabel, M.R., Mantoosh, S.M., Hopkins, J.J., Wagner, E.S., Gabaldon, T.A., and Zaharoff, D.A. (2020). Localized interleukin-12 for cancer immunotherapy. *Front. Immunol.* *11*, 575597.
20. Chakraborty, C., Sharma, A.R., Bhattacharya, M., and Lee, S.-S. (2021). From COVID-19 to cancer mRNA vaccines: moving from bench to clinic in the vaccine landscape. *Front. Immunol.* *12*, 679344.
21. Zeng, C., Zhang, C., Walker, P.G., and Dong, Y. (2020). Formulation and delivery technologies for mRNA vaccines. *Curr. Top. Microbiol. Immunol.* https://doi.org/10.1007/82_2020_217.
22. Smerdou, C., and Liljestrom, P. (1999). Non-viral amplification systems for gene transfer: vectors based on alphaviruses. *Curr. Opin. Mol. Ther.* *1*, 244–251.
23. Ballesteros-Briones, M.C., Silva-Pilipich, N., Herrador-Cañete, G., Vanrell, L., and Smerdou, C. (2020). A new generation of vaccines based on alphavirus self-amplifying RNA. *Curr. Opin. Virol.* *44*, 145–153.
24. Lundstrom, K. (2020). Semliki Forest virus-based immunotherapy for cancer. *Expert Opin. Biol. Ther.* *20*, 593–599.
25. Rodríguez-Madoz, J.R., Prieto, J., and Smerdou, C. (2005). Semliki forest virus vectors engineered to express higher IL-12 levels induce efficient elimination of murine colon adenocarcinomas. *Mol. Ther.* *12*, 153–163.
26. Rodríguez-Madoz, J.R., Liu, K.H., Quetglas, J.I., Ruiz-Guillen, M., Otano, I., Crettaz, J., Butler, S.D., Bellezza, C.A., Dykes, N.L., Tennant, B.C., et al. (2009). Semliki forest virus expressing interleukin-12 induces antiviral and antitumoral responses in woodchucks with chronic viral hepatitis and hepatocellular carcinoma. *J. Virol.* *83*, 12266–12278.
27. Chikkanna-Gowda, C.P., Sheahan, B.J., Fleeton, M.N., and Atkins, G.J. (2005). Regression of mouse tumours and inhibition of metastases following administration of a Semliki Forest virus vector with enhanced expression of IL-12. *Gene Ther.* *12*, 1253–1263.
28. Quetglas, J.I., Rodríguez-Madoz, J.R., Bezunartea, J., Ruiz-Guillen, M., Casales, E., Medina-Echeverez, J., Prieto, J., Berraondo, P., Hervás-Stubbs, S., and Smerdou, C. (2013). Eradication of liver-implanted tumors by Semliki Forest virus expressing IL-12 requires efficient long-term immune responses. *J. Immunol.* *190*, 2994–3004.
29. Rodríguez-Madoz, J.R., Zabala, M., Alfaro, M., Prieto, J., Kramer, M.G., and Smerdou, C. (2014). Short-term intratumoral interleukin-12 expressed from an alphaviral vector is sufficient to induce an efficient antitumoral response against spontaneous hepatocellular carcinomas. *Hum. Gene Ther.* *25*, 132–143.
30. Satkauskas, S., Bureau, M.F., Puc, M., Mahfoudi, A., Scherman, D., Miklavcic, D., and Mir, L.M. (2002). Mechanisms of in vivo DNA electrotransfer: respective contributions of cell electroporation and DNA electrophoresis. *Mol. Ther.* *5*, 133–140.
31. Bureau, M.F., Gehl, J., Deleuze, V., Mir, L.M., and Scherman, D. (2000). Importance of association between permeabilization and electrophoretic forces for intramuscular DNA electrotransfer. *Biochim. Biophys. Acta* *1474*, 353–359.
32. Roos, A.-K., Eriksson, F., Walters, D.C., Pisa, P., and King, A.D. (2009). Optimization of skin electroporation in mice to increase tolerability of DNA vaccine delivery to patients. *Mol. Ther.* *17*, 1637–1642.
33. Huysmans, H., Zhong, Z., De Temmerman, J., Mui, B.L., Tam, Y.K., Mc Cafferty, S., Gitsels, A., Vanrompay, D., and Sanders, N.N. (2019). Expression kinetics and innate immune response after electroporation and LNP-mediated delivery of a self-amplifying mRNA in the skin. *Mol. Ther. Nucleic Acids* *17*, 867–878.
34. André, F.M., Gehl, J., Sersa, G., Prétat, V., Hojman, P., Eriksen, J., Golzio, M., Cemazar, M., Pavselj, N., Rols, M.-P., et al. (2008). Efficiency of high and low voltage pulse combinations for gene electrotransfer in muscle, liver, tumor, and skin. *Hum. Gene Ther.* *19*, 1261–1271.
35. Johansson, D.X., Ljungberg, K., Kakoulidou, M., and Liljestrom, P. (2012). Intradermal electroporation of naked replicon RNA elicits strong immune responses. *PLoS One* *7*, e29732.
36. Huysmans, H., De Temmerman, J., Zhong, Z., Mc Cafferty, S., Combes, F., Haesebrouck, F., and Sanders, N.N. (2019). Improving the repeatability and efficacy of intradermal electroporated self-replicating mRNA. *Mol. Ther. Nucleic Acids* *17*, 388–395.
37. Heinzel, F.P., Hujer, A.M., Ahmed, F.N., and Nerko, R.M. (1997). In vivo production and function of IL-12 p40 homodimers. *J. Immunol.* *158*, 4381–4388.
38. Tammi, R.H., Kultti, A., Kosma, V.-M., Pirinen, R., Auvinen, P., and Tammi, M.I. (2008). Hyaluronan in human tumors: pathobiological and prognostic messages from cell-associated and stromal hyaluronan. *Semin. Cancer Biol.* *18*, 288–295.
39. Shepard, H.M. (2015). Breaching the castle walls: hyaluronan depletion as a therapeutic approach to cancer therapy. *Front. Oncol.* *5*, 192.
40. Thompson, C.B., Shepard, H.M., O'Connor, P.M., Kadhim, S., Jiang, P., Osgood, R.J., Bookbinder, L.H., Li, X., Sugarman, B.J., Connor, R.J., et al. (2010). Enzymatic depletion of tumor hyaluronan induces antitumor responses in preclinical animal models. *Mol. Cancer Ther.* *9*, 3052–3064.
41. Provenzano, P.P., Cuevas, C., Chang, A.E., Goel, V.K., Von Hoff, D.D., and Hingorani, S.R. (2012). Enzymatic targeting of the stroma ablates physical barriers to treatment of pancreatic ductal adenocarcinoma. *Cancer Cell* *21*, 418–429.
42. Jacobetz, M.A., Chan, D.S., Neesse, A., Bapiro, T.E., Cook, N., Frese, K.K., Feig, C., Nakagawa, T., Caldwell, M.E., Zecchini, H.I., et al. (2013). Hyaluronan impairs vascular function and drug delivery in a mouse model of pancreatic cancer. *Gut* *62*, 112–120.
43. Zhou, H., Fan, Z., Deng, J., Lemons, P.K., Arhontoulis, D.C., Bowne, W.B., and Cheng, H. (2016). Hyaluronidase embedded in nanocarrier PEG shell for enhanced tumor penetration and highly efficient antitumor efficacy. *Nano Lett.* *16*, 3268–3277.
44. Gong, H., Chao, Y., Xiang, J., Han, X., Song, G., Feng, L., Liu, J., Yang, G., Chen, Q., and Liu, Z. (2016). Hyaluronidase to enhance nanoparticle-based photodynamic tumor therapy. *Nano Lett.* *16*, 2512–2521.
45. Guan, X., Lin, L., Chen, J., Hu, Y., Sun, P., Tian, H., Maruyama, A., and Chen, X. (2019). Efficient PD-L1 gene silencing promoted by hyaluronidase for cancer immunotherapy. *J. Control. Release* *293*, 104–112.
46. Cemazar, M., Golzio, M., Sersa, G., Escoffre, J.-M., Coer, A., Vidic, S., and Teissie, J. (2012). Hyaluronidase and collagenase increase the transfection efficiency of gene electrotransfer in various murine tumors. *Hum. Gene Ther.* *23*, 128–137.
47. Quetglas, J.I., Labiano, S., Aznar, M.Á., Bolaños, E., Azpilikueta, A., Rodríguez, I., Casales, E., Sánchez-Paulete, A.R., Segura, V., Smerdou, C., et al. (2015).

- Virotherapy with a semliki forest virus-based vector encoding IL12 synergizes with PD-1/PD-L1 blockade. *Cancer Immunol. Res.* 3, 449–454.
48. Machado, B.A.S., Hodel, K.V.S., Fonseca, L.M.D.S., Mascarenhas, L.A.B., Andrade, L.P.C.d.S., Rocha, V.P.C., Soares, M.B.P., Berglund, P., Duthie, M.S., Reed, S.G., et al. (2021). The importance of RNA-based vaccines in the fight against COVID-19: an overview. *Vaccines* 9, 1345.
 49. Erasmus, J.H., Khandhar, A.P., O'Connor, M.A., Walls, A.C., Hemann, E.A., Murapa, P., Archer, J., Leventhal, S., Fuller, J.T., Lewis, T.B., et al. (2020). An Alphavirus-derived replicon RNA vaccine induces SARS-CoV-2 neutralizing antibody and T cell responses in mice and nonhuman primates. *Sci. Transl. Med.* 12, eabc9396.
 50. McKay, P.F., Hu, K., Blakney, A.K., Samnuan, K., Brown, J.C., Penn, R., Zhou, J., Bouton, C.R., Rogers, P., Polra, K., et al. (2020). Self-amplifying RNA SARS-CoV-2 lipid nanoparticle vaccine candidate induces high neutralizing antibody titers in mice. *Nat. Commun.* 11, 3523.
 51. Quetglas, J.I., Ruiz-Guillen, M., Aranda, A., Casales, E., Bezunartea, J., and Smerdou, C. (2010). Alphavirus vectors for cancer therapy. *Virus Res.* 153, 179–196.
 52. Ballesteros-Briones, M.C., Martisova, E., Casales, E., Silva-Pilipich, N., Buñuales, M., Galindo, J., Mancheño, U., Gorraiz, M., Lasarte, J.J., Kochan, G., et al. (2019). Short-term local expression of a PD-L1 blocking antibody from a self-replicating RNA vector induces potent antitumor responses. *Mol. Ther.* 27, 1892–1905.
 53. Komdeur, F.L., Singh, A., van de Wall, S., Meulenberg, J.J.M., Boerma, A., Hoogeboom, B.N., Paijens, S.T., Oyarce, C., de Bruyn, M., Schuurin, E., et al. (2021). First-in-Human phase I clinical trial of an SFV-based RNA replicon cancer vaccine against HPV-induced cancers. *Mol. Ther.* 29, 611–625.
 54. Simmerman, E., Chung, J., Lawson, A., and Kruse, E. (2020). Application of irreversible electroporation ablation as adjunctive treatment for margin enhancement: safety and efficacy. *J. Surg. Res.* 246, 260–268.
 55. Ganesh, S., Gonzalez-Edick, M., Gibbons, D., Van Roey, M., and Jooss, K. (2008). Intratumoral coadministration of hyaluronidase enzyme and oncolytic adenoviruses enhances virus potency in metastatic tumor models. *Clin. Cancer Res.* 14, 3933–3941.
 56. Weber, G.C., Buhren, B.A., Schrupf, H., Wohlrab, J., and Gerber, P.A. (2019). Clinical applications of hyaluronidase. *Adv. Exp. Med. Biol.* 1148, 255–277.
 57. Juneja, V.R., McGuire, K.A., Manguso, R.T., LaFleur, M.W., Collins, N., Haining, W.N., Freeman, G.J., and Sharpe, A.H. (2017). PD-L1 on tumor cells is sufficient for immune evasion in immunogenic tumors and inhibits CD8 T cell cytotoxicity. *J. Exp. Med.* 214, 895–904.
 58. Rodriguez-Madoz, J.R., Prieto, J., and Smerdou, C. (2007). Biodistribution and tumor infectivity of semliki forest virus vectors in mice: effects of re-administration. *Mol. Ther.* 15, 2164–2171.
 59. Liljeström, P., and Garoff, H. (2001). Expression of proteins using Semliki Forest virus vectors. *Curr. Protoc. Mol. Biol.* Chapter 16, 20.
 60. Smerdou, C., and Liljeström, P. (1999). Two-helper RNA system for production of recombinant semliki forest virus particles. *J. Virol.* 73, 1092–1098.
 61. Fleeton, M.N., Sheahan, B.J., Gould, E.A., Atkins, G.J., and Liljeström, P. (1999). Recombinant Semliki Forest virus particles encoding the prME or NS1 proteins of louping ill virus protect mice from lethal challenge. *J. Gen. Virol.* 80, 1189–1198.